

# Severe Fermi Surface Reconstruction at a Metamagnetic-Transition in $\text{Ca}_{2-x}\text{Sr}_x\text{RuO}_4$ (for $0.2 \leq x \leq 0.5$ )

L. Balicas,<sup>1</sup> S. Nakatsuji,<sup>2</sup> D. Hall,<sup>3</sup> H. Lee,<sup>4</sup> Z. Fisk<sup>4</sup>, Y. Maeno<sup>2</sup>, and D. J. Singh<sup>5</sup>

<sup>1</sup>National High Magnetic Field Laboratory, Florida State University, Tallahassee-FL 32306, USA

<sup>2</sup>Department of Physics, Graduate School of Science Kyoto University, Kyoto 606-8502, Japan

<sup>3</sup>American Physical Society, 1 Research Road, P. O. Box 9000, Ridge, NY, 11961.

<sup>4</sup>Department of Physics, University of California, Davis, California, 95916 and

<sup>5</sup>Condensed Matter Sciences Division, Oak Ridge National Laboratory, Oak Ridge, TN 37831-6032  
(Dated: December 25, 2021)

We report an electrical transport study in  $\text{Ca}_{2-x}\text{Sr}_x\text{RuO}_4$  single crystals at high magnetic fields ( $B$ ). For  $x = 0.2$ , the Hall constant  $R_{xy}$  decreases sharply at an anisotropic metamagnetic (MM) transition reaching its value for  $\text{Sr}_2\text{RuO}_4$  at high fields. A sharp decrease in the  $A$  coefficient of the resistivity  $T^2$ -term and a change in the structure of the angular magnetoresistance oscillations (AMRO) for  $B$  rotating in the planes, confirms the reconstruction of the Fermi surface (FS). Our observations and LDA calculations indicate a strong dependence of the FS on the Ca concentration and suggest the coexistence of itinerant and localized electronic states in single layered ruthenates.

PACS numbers: 72.15.-v, 71.30.+h, 72.15.Gd, 72.25.Ba

The single layered ruthenates  $\text{Ca}_{2-x}\text{Sr}_x\text{RuO}_4$  have a quite complex phase-diagram as function of doping  $x$  [1, 2]. While  $\text{Sr}_2\text{RuO}_4$  is a rare example of a well-defined two-dimensional Fermi liquid (FL) [3, 4] displaying spin-triplet superconductivity, the complete replacement of Sr by the isovalent element Ca produces to the Mott insulator  $\text{Ca}_2\text{RuO}_4$  [1, 5]. A series of correlated metallic states are protruded between both extremes.

In this system the relevant  $4d$ -orbitals belong to the  $t_{2g}$ -subshell and are degenerate. The planar structure conducts to very weak hybridization between orbitals which have either even ( $d_{xy}$ ) or odd ( $d_{yz}, d_{zx}$ ) parity under the reflection  $z \rightarrow -z$ . These orbitals lead in  $\text{Sr}_2\text{RuO}_4$  to a Fermi surface composed by three warped cylinders [6]. The  $\alpha$  and  $\beta$  sheets arise from 1D chains of  $d_{yz}, d_{zx}$  orbitals while the  $\gamma$  FS sheet originates from a 2D network of planar  $d_{xy}$  orbitals. Starting from the undistorted  $\text{Sr}_2\text{RuO}_4$ , Ca substitution initially stabilizes the rotation of  $\text{RuO}_6$  octahedra. This induces an enhancement of both the low  $T$  magnetic susceptibility  $\chi(T)$  and the Sommerfeld coefficient characterizing the electronic contribution to the specific heat [7]. Both quantities display a pronounced maximum at a critical value  $x_c = 0.5$  where the crystallographic structure of the  $\text{Ca}_{2-x}\text{Sr}_x\text{RuO}_4$  series changes from tetragonal to orthorhombic through a second-order structural transition [1]. For stronger Ca concentrations and as we approach the Mott transition at  $x \lesssim 0.2$ ,  $\chi(T)$  is strongly suppressed by the emergence of AF correlations.

This complex evolution has led to various theoretical proposals, in particular to the idea that some of the  $d$ -orbitals display localized spin and orbital degrees of freedom, while others provide itinerant carriers. This so-called orbital-selective Mott transition (OSMT) [8] could, for instance, explain the experimental observation of an effective spin  $S$  very close to the value  $1/2$

for  $0.2 \leq x \leq 0.5$  [7] which is difficult to understand within an entirely itinerant description. However the concept of orbital-selective Mott-transition was challenged by the dynamical mean field (DMFT) calculations of Liebsch [9] which suggest that two bands of different widths coupled by electron-electron interactions always undergo a single simultaneous Mott transition. Koga *et al.* claim that this apparent discrepancy can be solved by taking into account a finite Hund coupling in Hubbard models considering multiple bands with different bandwidths [10]. In contrast, according to Okamoto and Millis [11] Hund coupling would in fact stabilize a given system against orbital ordering preventing the occurrence of the OSMT. Finally, a recent photoemission study in  $\text{Ca}_{1.5}\text{Sr}_{0.5}\text{RuO}_4$  finds that the geometry of the  $\alpha$  and  $\beta$  FS sheets remains almost unchanged respect to  $\text{Sr}_2\text{RuO}_4$ , with the  $\gamma$  sheet exhibiting a hole-like FS in contrast to being electron-like in the pure Sr compound [12]. The observation of *all* three volume conserving FS sheets would demonstrate the absence of OSMT in  $\text{Ca}_{1.5}\text{Sr}_{0.5}\text{RuO}_4$ .

To clarify the possible existence of localized carriers within a metallic  $d$ -electron system as proposed by the orbital-selective Mott-transition model, we performed a detailed electrical transport study at high magnetic fields in  $\text{Ca}_{2-x}\text{Sr}_x\text{RuO}_4$  single crystals for  $x = 0.2$  and  $0.5$ . In particular, we studied the Hall effect and the angular dependence of the magnetoresistance or AMRO, which is a technique commonly used to define the relatively simple two-dimensional (2D) FS of layered organic metals [13], and which has already provided valuable information about the FS of  $\text{Sr}_2\text{RuO}_4$  [14, 15]. Our measurements reveal a profound modification of the original FS of  $\text{Sr}_2\text{RuO}_4$  upon Ca doping and a severe reconstruction of the FS of  $x = 0.2$  at a metamagnetic transition. These observations are consistent with the proposed existence of localized  $d$ -electronic states in  $\text{Ca}_{2-x}\text{Sr}_x\text{RuO}_4$

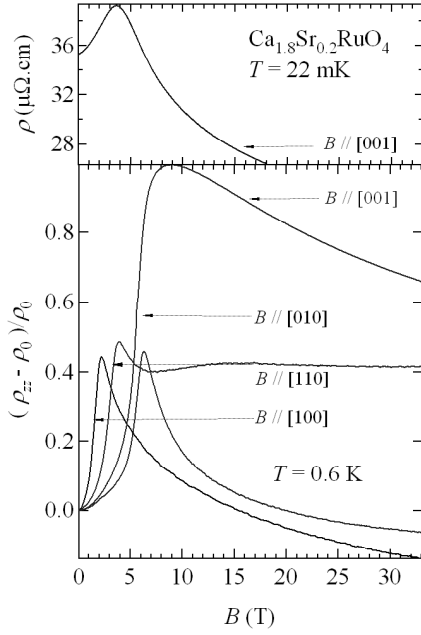


FIG. 1: Upper panel: In-plane resistivity  $\rho$  for a  $\text{Ca}_{1.8}\text{Sr}_{0.2}\text{RuO}_4$  single crystal as a function of the field  $B$  applied along the inter-plane direction at  $T = 22$  mK. Lower panel: Inter-plane resistivity  $\rho_{zz}$  normalized respect to its zero field value  $\rho_0$ , as a function of the external field  $B$  oriented along different crystallographic orientations and at  $T \approx 0.6$ . In both panels a pronounced peak is observed at an anisotropic metamagnetic transition.

(for  $0.2 \leq x \leq 0.5$ ).

The upper panel of Fig. 1 shows the in-plane resistivity of  $\text{Ca}_{1.8}\text{Sr}_{0.2}\text{RuO}_4$  single crystal at  $T = 22$  mK and as a function of the field  $B$  applied along the inter-plane direction. While the lower panel of Fig. 1 shows the relative change of its inter-plane resistivity  $(\rho_{zz} - \rho_0)/\rho_0$  (where  $\rho_0$  is the residual resistivity at  $B = 0$ ) as a function of  $B$  at  $T = 600$  mK and for four orientations respect to  $B$  (as indicated in the figure). For all orientations both  $\rho$  and  $\rho_{zz}$  display pronounced positive magnetoresistivity preceding a sharp peak beyond which the system displays a remarkable negative magnetoresistance (the exact position in  $B$  is sample dependent). Notice how  $\rho$  at high fields decreases beyond its value at  $B = 0$ . This peak is produced by a metamagnetic (MM) transition, i.e., a rapid increase in magnetization between two distinct paramagnetic states, the first one characterized by short-range antiferromagnetic correlations and the second one dominated by ferromagnetic-like interactions [7]. Both, the position of the metamagnetic critical field  $B_{\text{MM}}$  (as defined by the peak in the resistivity) as well as the background magnetoresistivity display a remarkable orientation dependence.

The color plot in Fig. 2(a) shows the exponent  $n = \partial \ln(\rho - \rho_0)/\partial(T)$  of the in-plane resistivity  $\rho$  in a limited range of the  $T - B$  space. The purple regions emerg-

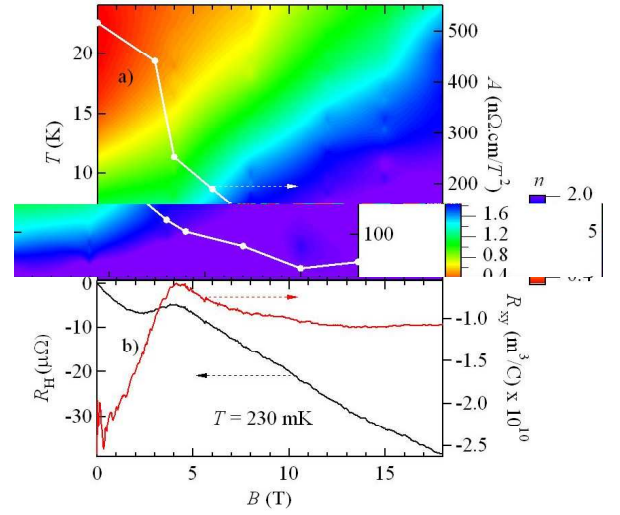


FIG. 2: a) The exponent  $n = \partial \ln(\rho - \rho_0)/\partial(T)$  of the in-plane resistivity  $\rho$  in the  $B - T$  plane. The Fermi-liquid ground state is always observed at lower  $T$ s. The white symbols describe the evolution of the  $A = (\rho - \rho_0)/T^2$  coefficient as a function  $B$ . b) The Hall resistance  $R_H$  and the Hall constant  $R_{xy}$  as a function of  $B$  at  $T = 230$  mK. Notice the sharp decrease in  $R_{xy}$  at the metamagnetic transition.

ing at low temperatures reveal the existence of a Fermi liquid (FL) ground state ( $n = 2$ ). Notice how the characteristic temperature  $T_{\text{FL}}$  below which FL-like behavior is observed increases with  $B$ . The white line and markers indicate the evolution in  $B$  of the resistivity's  $A = (\rho - \rho_0)/T^2$  coefficient which shows a pronounced decrement at the transition. At  $B = 0$ ,  $A$  is proportional to the square of the density of states at the Fermi level  $\rho(\epsilon_F)^2$  via the Kadowaki-Woods ratio. This reduction in  $\rho(\epsilon_F)$ , confirmed by heat capacity measurements [16], points towards a reconfiguration of the FS at the MM-transition. Furthermore, the decrease in  $A$  coupled to an increase in  $T_{\text{FL}}$  has usually been taken as an indication of the close proximity of a given system to a quantum critical point at  $B = 0$  [17], which in our case is probably associated with the Mott transition. The fact that  $A$  and  $T_{\text{FL}}$  as well as the lattice constants [18] change continuously with  $B$ , while  $\rho_{zz}$  shows a discontinuity at the metamagnetic transition suggests that it corresponds to a percolation-like first-order transition as proposed by Ref. [19]. Fig. 2(a) shows no evidence of critical behavior as expected for a first-order metamagnetic transition. While Fig. 2(b) shows the most relevant result of this study, the Hall resistance  $R_H = V_H/I$ , where  $V_H$  is the Hall voltage and  $I$  the electrical current, and the Hall constant  $R_{xy} = R_H \cdot t/B$ , where  $t$  is the sample thickness, as a function of  $B$  at  $T = 230$  mK. At such low  $T$ s, Ref. [20] has demonstrated that one reaches the elastic-scattering regime where  $R_H$  is determined mainly by the FS topography rather than by the details of the scatter-

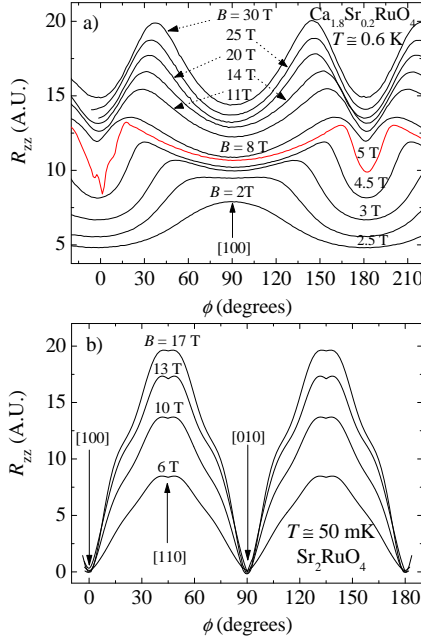


FIG. 3: a) Inter-plane resistance  $R_{zz}$  as a function of the angle  $\phi$  between  $B$  and an in-plane axis for a  $\text{Ca}_{1.8}\text{Sr}_{0.2}\text{RuO}_4$  single crystal at  $T = 0.6$  K. Notice how the low field two-fold periodicity progressively becomes four-fold at high fields after the metamagnetic transition is crossed. b)  $R_{zz}$  for a  $\text{Sr}_2\text{RuO}_4$  single crystal as function of the angle  $\phi$  and for several values of  $B$  and at  $T \approx 50$  mK. Notice the progressive emergence of a new periodicity at higher fields. In both graphs, all curves are vertically displaced for clarity.

ing mechanism. Notice how the absolute value of  $R_{xy}$  decreases through the metamagnetic transition from nearly  $2.5 \pm 0.5 \times 10^{-10} \text{ m}^3/\text{C}$  at very low fields and saturates at the value of  $\approx 1 \pm 0.05 \times 10^{-10} \text{ m}^3/\text{C}$ , which is precisely the value reported for  $\text{Sr}_2\text{RuO}_4$  [20]. This indicates an important modification of the original band structure of  $\text{Sr}_2\text{RuO}_4$  upon Ca doping as well as a severe reconstruction of the FS at the metamagnetic transition. The Hall mobility  $R_{xy}/\rho$  decreases rapidly from  $\sim 6.5 \text{ cm}^2/\text{Vs}$  at  $B = 0$  to a value of about  $\sim 1.5 \text{ cm}^2/\text{Vs}$  at  $B_{\text{MM}}$  saturating at high  $B$ s to a value of  $\sim 4.0 \text{ cm}^2/\text{Vs}$  reflecting an increase in scattering events. Thus, the increase in conductivity above the transition cannot be attributed to an increase in mobility, but it reflects perhaps the reduction in the effective mass of the charge carriers. Notice that in multi-band systems such as the ruthenates, whose FS may be composed by both electron and hole FS sheets,  $R_{xy}$  is no longer  $\propto n_c^{-1}$  where  $n_c$  is the number of charge carriers. Although the abrupt change in  $R_{xy}$  cannot be interpreted as a change in FS volume, this metamagnetic behavior bears similarities with the metamagnetism followed by colossal magnetoresistive-like behavior seen in the  $\text{Ca}_3\text{Ru}_2\text{O}_7$  system and which is ascribed to the destabilization of an orbital-ordered state [21]. Similarly, in

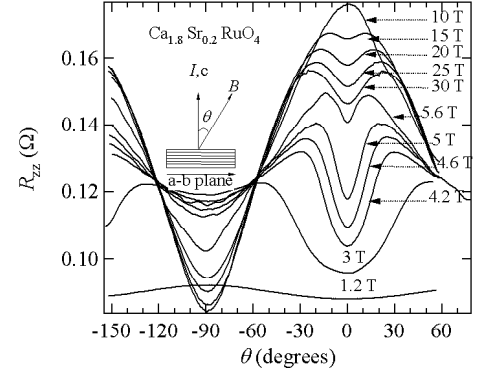


FIG. 4: Inter-plane resistance  $R_{zz}$  as a function of the angle  $\theta$  between the external magnetic field  $B$  and the inter-plane  $c$ -axis for a  $\text{Ca}_{1.8}\text{Sr}_{0.2}\text{RuO}_4$  single crystal at  $T = 0.6$  K.

our case it could also indicate the existence of localized  $d$ -electron states that are destabilized by the external field.

Figure 3(a) shows the inter-plane resistance  $R_{zz}$  of a  $\text{Ca}_{1.8}\text{Sr}_{0.2}\text{RuO}_4$  single crystal at  $T = 0.6$  K and as a function of the azimuthal angle  $\phi$  between  $B$  and an in-plane axis for several values of  $B$  below and above  $B_{\text{MM}}$  (as indicated in the figure). All curves are vertically displaced for clarity. At low fields,  $R_{zz}(\phi)$  is essentially two-fold. A similar magnetoresistive effect, but displaying four-fold periodicity (that reflects the angular symmetry of the  $\text{CuO}_2$  planes which leads to a four-fold modulation in  $k_F$ ,  $v_F$  and  $\tau$ ), was reported in the tetragonal compound  $\text{Ti}_2\text{Ba}_2\text{CuO}_6$  [22] as well as in  $\text{Sr}_2\text{RuO}_4$  [15]. Here, the two-fold sinusoidal-like dependence, which reflects the symmetry of the orthorhombic structure, progressively disappears as the MM-transition is approached. As  $B$  further increases a new, nearly four-fold, periodicity emerges. This unique evolution of the AMRO data across the MM-transition is consistent with the reconstruction of the FS revealed by  $R_{xy}$ . It cannot be simply explained in terms semiclassical orbits exploring the geometry of the FS in greater detail at higher fields. To illustrate this point in Fig. 3(b) we show  $R_{zz}(\phi)$  for a  $\text{Sr}_2\text{RuO}_4$  single crystal at  $T = 50$  mK and for several values of  $B$  (traces are vertically displaced for clarity). At lower  $B$ s one clearly observes the four-fold AMRO but as  $B$  increases its amplitude increases with a new periodicity emerging and *overlapping* it. The new structure reflecting the warping of the FS, does *not* emerge in detriment of the lower field one(s), contrary to the  $x = 0.2$  case. More importantly, even above the metamagnetic transition the symmetry of the FS for  $x = 0.2$  remains essentially two- and not four-fold.

A two-dimensional FS composed of three open cylinders, as seen by ARPES for  $x = 0.5$ , would generate a distinctive polar AMRO ( $\rho_{zz}(\theta, B)$  where  $\theta$  is the angle between  $B$  and the  $c$ -axis), as seen for instance, in  $\text{Sr}_2\text{RuO}_4$  [14]. For very low levels of disorder, one should observe

a series of peaks, periodic in  $\tan(\theta)$ , due to the Yamaji effect [23]. While for disordered systems one might observe only a small amplitude single sinusoidal component showing a minimum for  $B \parallel c$ -axis. Nevertheless, as seen in Fig. 4 which shows  $R_{zz}(\theta)$  at  $T = 0.6$  K and for several field values, a very pronounced AMRO is indeed observed for  $x = 0.2$  but it *does not* display an angular structure compatible with the above discussion. A quite similar but far less pronounced AMRO (as well as MM behavior) is observed also in  $x = 0.5$  (not shown here). The origin of the observed dependence remains unclear, although it is similar to that of the so-called Lebed oscillations seen in quasi-one-dimensional organic conductors [24]. Were this their correct description, it would imply that the 2D  $\gamma$  FS sheet has moved below  $\rho(\epsilon_F)$  while the  $\alpha$  and/or the  $\beta$  Q1D FS sheets would survive this level of doping. Quasi-one-dimensional FS sheets with a certain degree of nesting would explain the development of AF correlations and would be compatible with the two-fold azimuthal AMRO. Notice that according to Ref. [25] the rotation of the  $\text{RuO}_6$  octahedra is expected to seriously reduce the occupation of the  $\gamma$  band. In any case, this unusual polar AMRO implies that high levels of Ca doping modifies the original FS of  $\text{Sr}_2\text{RuO}_4$  at the point that it no longer reveals a clear 2D character, in sharp contrast with the ARPES measurements [12].

In order to understand the evolution of the FS as a function of Ca doping, LDA calculations were done using the LAPW method and the neutron crystal structures [18] of  $x = 0$  at 180 K (S0 short octahedra, Mott insulator), of  $x = 0$  at 400 K (L0, long octahedra, metal) and  $x = 0.5$  at 10 K (L5). For the S0 an antiferromagnetic state,  $m \sim 2\mu_B$  is predicted; the electronic structure has very narrow bands at  $E_F$ , favorable for the observed Mott insulating ground state. The L0 structure is an itinerant ferromagnet,  $m \sim 1\mu_B$  in the LDA. Electric field gradients (EFG) are sensitive probes of orbital occupation. A large change is found between the L0 and S0 structures: the average Ru EFG's are  $-4.9 \times 10^{21}$  V/m<sup>2</sup> and  $+4.3 \times 10^{21}$  V/m<sup>2</sup>, for paramagnetic L0 and antiferromagnetic S0, respectively. The L5 structure is weakly ferromagnetic, presumably due to neglect of quantum critical fluctuations in the LDA.  $x = 0.2$  is on the borderline between these two states, i.e. it is in a long octahedra structure intermediate between L0 and L5, is on the verge of the long to short crossover. The L0 FS is complex due to zone folding and lowered symmetry, but, it has two contributions, heavy bands (H), that do not contribute to transport and an itinerant component. The H-FS is strongly affected by magnetic ordering, seen in a reduction by a factor of more than 2 in the EFG (to  $-2.3 \times 10^{21}$  V/m<sup>2</sup>) when ferromagnetic, showing a change in orbital population. This is accompanied by a large change in the density of states:  $N(E_F) = 2.5$  eV<sup>-1</sup> per Ru per spin (paramagnetic) 1.3 eV<sup>-1</sup> (majority) and 2.9 eV<sup>-1</sup> (minority), even though the in-plane transport function  $Nv_x^2$ , which

reflects the itinerant sheets, is the same to better than 10% for the paramagnetic, ferromagnetic majority and ferromagnetic minority FS's. If the situation is the same at  $x=0.2$  as expected, the implication is that at the metamagnetic transition the heavy part of the FS is removed for majority carriers, consistent with the experimental results.

In summary, the Fermi surface of the  $\text{Ca}_{2-x}\text{Sr}_x\text{RuO}_4$  system is strongly dependent on  $x$ . The anomalous polar AMRO and the severe field-induced Fermi surface reconstruction observed at the metamagnetic transition of  $x = 0.2$ , could be evidence for localized  $d$ -electronic states within the metallic phase seen for  $0.2 \leq x \leq 0.5$ . This possibility is supported by our LDA calculations and is consistent with the predictions of the orbital-selective Mott-transition scenario.

We acknowledge useful discussions with M. Braden, P. Schlottmann, and P. B. Littlewood. LB acknowledges support from the NHMFL in-house program and ZF from NSF DMR 0433560. The NHMFL is supported by NSF-DMR-0084173. Work at Kyoto was supported in part by Grants-in-Aid for Scientific Research from JSPS and for the 21st Century COE "Center for Diversity and Universality in Physics" from MEXT of Japan.

- 
- [1] S. Nakatsuji, and Y. Maeno, Phys. Rev. Lett. **84**, 2666 (2000)
  - [2] S. Nakatsuji, and Y. Maeno, Phys. Rev. B **62**, 6458 (2000).
  - [3] Y. Maeno *et al.*, J. Phys. Soc. Jpn. **66**, 1405 (1997).
  - [4] A. P. Mackenzie *et al.*, Phys. Rev. Lett. **76** 3786 (1996).
  - [5] S. Nakatsuji *et al.*, J. Phys. Soc. Jpn. **66**, 1868 (1997).
  - [6] C. Bergemann, *et al.*, and Y. Maeno, Phys. Rev. Lett. **84**, 2662 (2000) and references therein.
  - [7] S. Nakatsuji *et al.*, Phys. Rev. Lett. **90**, 137202 (2003).
  - [8] V. I. Anisimov *et al.*, Eur. Phys. J B **25**, 191 (2002).
  - [9] A. Liebsch, Phys. Rev. Lett. **91**, 226401 (2003); Europhys. Lett. **63**, 97 (2003); Phys. Rev. B **70**, 165103 (2004).
  - [10] A. Koga, N. Kawakami, T. M. Rice, and M. Sigrist, Phys. Rev. Lett. **92**, 216402 (2004).
  - [11] S. Okamoto and A. J. Millis, Phys. Rev. B **70**, 195120 (2004).
  - [12] S. C. Wang, *et al.*, Phys. Rev. Lett. **93**, 177007 (2004).
  - [13] T. Ishiguro, K. Yamaji, *Organic Superconductors*, (Springer, Berlin, 1990); J. Wosnitzer, *Fermi Surfaces of Low-dimensional Organic Metals and Superconductors*, (Springer, Berlin, 1996).
  - [14] E. Ohmichi, *et al.*, Phys. Rev. B **59**, 7263 (1999).
  - [15] E. Ohmichi, *et al.*, Phys. Rev. B **61**, 7101 (2000).
  - [16] M. Braden, private communication.
  - [17] S. Y. Li, *et al.*, Phys. Rev. Lett. **93**, 056401 (2004).
  - [18] M. Kriener *et al.*, cond-mat/0408015.
  - [19] M. Sigrist and M. Troyer, Eur. Phys. J. B **39**, 207 (2004).
  - [20] L. M. Galvin, R. S. Perry, A. W. Tyler, and A. P. Mackenzie, Phys. Rev. B **63**, 161102(R) (2001).
  - [21] J. F. Karpus, *et al.*, Phys. Rev. Lett. **93**, 167205 (2004);

- X. N. Lin, *et al.*, *ibid* **95**, 017203 (2005).
- [22] N. E. Hussey *et al.*, Phys. Rev. Lett. **76**, 122 (1996).
- [23] K. Yamaji, J. Phys. Soc. Jpn. **58**, 1520 (1989).
- [24] A. G. Lebed, N. N. Bagmet and M. J. Naughton, Phys. Rev. Lett. **93**, 157006 (2004).
- [25] Z. Fang, N. Nagaosa, and K. Terakura, Phys. Rev. B **69**, 045116 (2004).